SVEP1 regulates GPCR-mediated vasoconstriction via integrin α9β1 and α4β1

Gavin Morris[1], Elisavet Karamanavi[1], Matthew Denniff[1], Sarah Andrews[1], Renata Kostogrys[2], Vasiliki Bountziouka[1], Maryam Ghaderi-Najafabadi[1], Noor Shamkhi[1], George McConnell[1], Michael Kaiser[1], Christine Schofield[3], Thorsten Kessler[4], Richard Rainbow[5], Nilesh Samani[1], and Thomas Webb[1]

[1]University of Leicester
[2]University of Agriculture in Krakow
[3]Horizon Discovery Group plc
[4]German Heart Centre Munich
[5]University of Liverpool

April 16, 2024

Abstract

Background and purpose Vascular tone is regulated by the relative contractile state of vascular smooth muscle cells (VSMCs). Several integrins directly modulate VSMC contraction by regulating calcium influx through L-type voltage-gated Ca2+ channels (VGCCs). Genetic variants in ITGA9, which encodes the α9 subunit of integrin α9β1, and SVEP1, a ligand for integrin α9β1, associate with elevated blood pressure, however, neither SVEP1 nor integrin α9β1 have reported roles in vasoregulation. We therefore determined whether SVEP1 and integrin α9β1 can regulate VSMC contraction. Experimental Approach SVEP1 and integrin binding were confirmed by immunoprecipitation and cell binding assays. Human induced pluripotent stem cell-derived VSMCs were used in in vitro [Ca2+]i studies, and aortas from a Svep1+/- knockout mouse model were used in wire myography to measure vessel contraction. Key Results We confirmed the ligation of SVEP1 to integrin α9β1 and additionally found SVEP1 to directly bind to integrin α4β1. Inhibition of SVEP1, integrin α4β1 or α9β1 significantly enhanced [Ca2+]i release in isolated VSMCs to Gαq/11-vasoconstrictors. This response was confirmed in whole vessels where a greater contraction to U46619 was seen in vessels from Svep1+/- mice compared to littermate controls or when integrin α4β1 or α9β1 were inhibited. Inhibition studies suggested that this effect was mediated via VGCCs in a PKC dependent mechanism. Conclusions and Implications Our studies reveal a novel role for SVEP1 and the integrins α4β1 and α9β1 in reducing vascular hyper-contractility. This could provide an explanation for the genetic associations with blood pressure risk at the SVEP1 and ITGA9 loci.

Σ̈ΕΠ1 ρεγυλατες ΓΠ̂Ρ-μεδιατεδ ασοςονστριςτιον ια ιντεγριν α9β1 ανδ α4β1

Morris GE[1*], Karamanavi E[1], Denniff MJ[1], Andrews SA[1], Kostogrys RB[2], Bountziouka V[1], Ghaderi-Najafabadi M[1], Shamkhi N[1], McConnell G[1], Kaiser MA[1], Carleton L[3], Schofield C[3], Kessler T[4,5], Rainbow RD[6], Samani, NJ[1], Webb TR[1].

Author Affiliation and email address:

1 Department of Cardiovascular Sciences, University of Leicester and National Institute for Health Research Leicester Biomedical Research Centre, Glenfield Hospital, Leicester, LE3 9QP, United Kingdom.

2 Department of Human Nutrition, Faculty of Food Technology, University of Agriculture in Krakow, Poland (R.B.K.).

3 Horizon Discovery Ltd., 8100 Cambridge Research Park, Cambridge, CB25 9TL, United Kingdom.

4 Department of Cardiology, German Heart Centre Munich, Technical University of Munich, Munich, Germany.

5 German Centre of Cardiovascular Research (DZHK e. V.), Partner Site Munich Heart Alliance, Munich, Germany.

6 Department of Cardiovascular and Metabolic Medicine & Liverpool Centre for Cardiovascular Science, University of Liverpool, Liverpool, L69 3GE.

Morris GE: gem8@leicester.ac.uk, Karamanavi E: eliskaram@gmail.com,

Denniff MJ: md123@leicester.ac.uk, Andrews SA: sa619@leicester.ac.uk,

Kostogrys RB: rkostogrys@gmail.com, Bountziouka V: vb134@leicester.ac.uk,

Ghaderi-Najafabadi M: mg874@cam.ac.uk,

Shamkhi N: noor.shamkhi@bioch.ox.ac.uk,

McConnell G: gm307@leicester.ac.uk, Kaiser MA: zc3hc1@gmail.com

Carleton L: laura.carleton@horizondiscovery.com,

Schofield C: christine.schofield@horizondiscovery.com,

Kessler T: thorsten.kessler@tum.de, Rainbow RD: richard.rainbow@liverpool.ac.uk,

Samani NJ: njs@leicester.ac.uk, Webb TR: trw126@leicester.ac.uk.

*** Corresponding Author:** Gavin Morris, email:*gem8@leicester.ac.uk* , telephone: +44(0)116 2044763, address: Department of Cardiovascular Sciences, University of Leicester and National Institute for Health Research Leicester Biomedical Research Centre, Glenfield Hospital, Leicester, LE3 9QP, United Kingdom. ORCID: 0000-0003-4054-6959.

Keywords

SVEP1, integrin α4β1, integrin α9β1, blood pressure, vasoconstriction.

Acknowledgements

We thank Professor Shigeyuki Kon at Fukuyama University for providing us with the anti-integrin α9 antibody (55A2C). We acknowledge the staff in the University of the Leicester Division of Biomedical Services for technical expertise and animal care. We thank the Advanced Imaging Facility (RRID:SCR_020967) at the University of Leicester for support.

Source of Funding

The research presented here has received funding from the British Heart Foundation (PG/20/10056 and SP16/4/32697), the European Union Seventh Framework Programme FP7/2007-2013 under grant agreement number HEALTH-F2-2013-601456, the van Geest Heart and Cardiovascular Diseases Research Fund, administered by the Department of Cardiovascular Sciences, University of Leicester.

Competing interests

The authors declare no competing interests.

Disclosures

None

Data availability Statement

The data supporting the findings in this study are available from the corresponding author upon reasonable request. Some data may not be available because of privacy or ethical restrictions.

Author Contribution Statement

G.E.M and T.R.W conceived the study and participated in the overall design, and coordination of the study. G.E.M designed and performed*in vitro* experiments. S.A.A performed the immunoprecipitation and cell binding studies. E.K and R.B.K performed IHC analysis. E.K and M.J.D performed wire myography experiments, with R.D.R and T.K providing support and supervision for the *ex vivo* models, and V. B providing statistical support. G.E.M, G.M, N.M.G, N.S, M.A.K, L.C, C.S, and T.R.W designed and generated the SVEP1 knockout iPSC lines. G.E.M., N.J.S. and T.R.W supervised the overall project. G.E.M and T.R.W wrote the manuscript. All authors reviewed the manuscript.

Ethics Approval Statement

Animal experimentation was approved by the local animal ethics committee and performed according to ARRIVE (Animal Research: Reporting of In Vivo Experiments) guidelines and under United Kingdom Home Office Project Licence (P4E9A1CCA).

ABSTRACT

Background and purpose

Vascular tone is regulated by the relative contractile state of vascular smooth muscle cells (VSMCs). Several integrins directly modulate VSMC contraction by regulating calcium influx through L-type voltage-gated Ca^{2+} channels (VGCCs). Genetic variants in*ITGA9* , which encodes the α9 subunit of integrin α9β1, and*SVEP1* , a ligand for integrin α9β1, associate with elevated blood pressure, however, neither SVEP1 nor integrin α9β1 have reported roles in vasoregulation. We therefore determined whether SVEP1 and integrin α9β1 can regulate VSMC contraction.

Experimental Approach

SVEP1 and integrin binding were confirmed by immunoprecipitation and cell binding assays. Human induced pluripotent stem cell-derived VSMCs were used in *in vitro*$[Ca^{2+}]_i$ studies, and aortas from a*Svep1*$^{+/-}$ knockout mouse model were used in wire myography to measure vessel contraction.

Key Results

We confirmed the ligation of SVEP1 to integrin α9β1 and additionally found SVEP1 to directly bind to integrin α4β1. Inhibition of SVEP1, integrin α4β1 or α9β1 significantly enhanced $[Ca^{2+}]_i$ release in isolated VSMCs to $G\alpha_{q/11}$-vasoconstrictors. This response was confirmed in whole vessels where a greater contraction to U46619 was seen in vessels from *Svep1*$^{+/-}$ mice compared to littermate controls or when integrin α4β1 or α9β1 were inhibited. Inhibition studies suggested that this effect was mediated via VGCCs in a PKC dependent mechanism.

Conclusions and Implications

Our studies reveal a novel role for SVEP1 and the integrins α4β1 and α9β1 in reducing vascular hypercontractility. This could provide an explanation for the genetic associations with blood pressure risk at the*SVEP1 and ITGA9* loci.

Word count: 273

What is already known

Genetic variants in *SVEP1* associate with elevated blood pressure.

What this study adds

SVEP1 is a new regulator of vasoconstriction.

Clinical significance

SVEP1 is a potential therapeutic candidate in vascular hypertension.

Activation of integrin α9β1 could provide a new treatment in vascular hypertension.

Non-standard Abbreviations

ADAM a disintegrin and metalloproteinase with thrombospondin motifs

ADAMTS-7 ADAM Metallopeptidase With Thrombospondin Type 1 Motif 7

bFGF basic fibroblast growth factor

BOP*N* -(Benzenesulfonyl)-L-prolyl-L-*O* -(1-pyrrolidinylcarbonyl)tyrosine

Ca^{2+} calcium ion

CAD coronary artery disease

CAEC coronary artery endothelial cell

Cch carbachol

CCP complement control protein

c-SRC proto-oncogene tyrosine-protein kinase Src

CRISPR clustered regularly interspaced short palindromic repeats

EC endothelial cell

ECM extracellular matrix

EGF epidermal growth factor

ET-1 endothelin-1

GFR growth factor reduced

GPCR G protein coupled receptor

HEK human embryonic kidney

HUVEC human umbilical vein endothelial cell

IP3 inositol 1,4,5-trisphosphate

iPSC induced pluripotent stem cell

KO knockout

MLCK myosin light chain kinase

NTC non-targeting control

PDGF platelet-derived growth factor

PIP2 phosphatidylinositol 4,5-bisphosphate

PKC protein kinase C

PLC phospholipase C

PE phenylephrine

SD standard deviation

siRNA small interfering RNA

SVEP1 Sushi, von Willebrand factor type A, EGF and pentraxin domain-containing protein 1

TGF transforming growth factor

UTP uridine-5'-triphosphate

VGCC L-type voltage-gated calcium channel

VSMC vascular smooth muscle cell

WT wild-type

INTRODUCTION

Arterial diseases including hypertension and coronary artery disease (CAD) display a degree of dysregulation in the contractile behaviour of the smooth muscle. Vascular tone is regulated by the relative contractile state of vascular smooth muscle cells (VSMCs)[1,2]. VSMC contraction provides force generation through the phosphorylation of myosin light chain kinase (MLCK) which facilitates interaction between actin and myosin filaments. MLCK is directly phosphorylated by calcium-bound calmodulin. Increases in intracellular calcium concentrations ($[Ca^{2+}]_i$) occur through PKC-mediated activation of L-type voltage-gated calcium channels (VGCCs) leading to an influx of extracellular Ca^{2+} ions, or via activation of $G_{\alpha\chi}$-Protein Coupled Receptors (GPCRs) leading to PLCβ-mediated Ca^{2+} ion release from the sarcoplasmic reticulum. Whilst these central signalling pathways controlling contraction are widely characterised, modulation of these pathways remains ill-defined.

Several integrins can directly modulate vascular smooth muscle cell contraction by regulating calcium influx through VGCCs[3-7]. Within the airway, integrin α9β1 has been specifically identified as preventing exaggerated airway smooth muscle contraction, where conditional knockout of the α9 subunit in airway smooth muscle causes a spontaneous increase in pulmonary resistance in response to multiple GPCR agonists[8]. SVEP1, a high affinity ligand for integrin α9β1[9], is a 390 kDa secreted extracellular matrix (ECM) protein comprised of sushi (complement control protein (CCP)), von Willebrand factor type A, epidermal growth factor-like, and pentraxin domains[10]. The function of SVEP1 remains unclear but it has reported roles in cell adhesion[9-12], lymphatic vessel formation[13,14], epidermal differentiation[15], and cancer progression[16,17]. A low frequency coding variant rs111245230 (p.D2702G) within SVEP1 associates with elevated blood pressure (BP)[18] and CAD[19]. rs111245230 is situated adjacent to the binding motif through which SVEP1 binds to integrin α9β1[9]. Genetic variants associated with reduced expression of *ITGA9* , which encodes the α9 subunit of integrin α9β1, have also been reported to associate with increased BP[20,21]. Neither SVEP1 nor integrin α9β1 have a reported role in vasoregulation, however direct activation of integrin α4β1, with which integrin α9β1 forms an integrin subfamily[22], can induce VSMC contraction[4].

The role of SVEP1 in cardiovascular disease is only now beginning to be realised with two recent *in vivo* studies showing SVEP1 to be primarily expressed within blood vessels[23] and SVEP1 knockout affecting atherosclerosis development[23,24]. Due to the genetic association between variants in *SVEP1* and*ITGA9* with BP, the role of integrin α9β1 in airway contraction, and SVEP1 expression, we examined the role of these proteins in regulating VSMC contractility.

Results

Σ″ΕΠ1 βινδς το ιντεγριν α4β1 ανδ α9β1

SVEP1 is a known ligand for integrin α9β1, but whether SVEP1 can bind to the closely related integrin α4β1[22] has not been reported. Using immunoprecipitation we found SVEP1 to bind to integrin α4 (Fig. 1A), and confirmed the ligation of SVEP1 to integrin α9 (Fig. 1B). In addition to demonstrating the direct ligation of SVEP1 to integrin α4, we investigated how SVEP1 interacts with α4 using a cell adhesion assay. SVEP1 binds to integrin α9β1 through its CCP21 domain[9]. We coated tissue culture plastic with 100nM manose-binding protein (MBP), MBP-tagged CCP21 or CCP22 domain peptides. HEK293 cells overexpressing the

integrin α4 subunit bound to the CCP21 peptide significantly greater than either MBP (P <0.01) or CCP22 (P <0.05) control proteins (Fig. 1C). Similar results were seen for HEK293 cells overexpressing the integrin α9 subunit, with cells binding to the CCP21 domain significantly higher than MBP (P <0.01) or CCP22 (P <0.05) control proteins (Fig. 1D).

Σ″ΕΠ1, ιντεγριν α4β1ανδ α9β1 αρε εξπρεσσεδ ιν ασχυλαρ σμοοτη μυσχλε

We examined the gene expression of *SVEP1* , *ITGA4* and*ITGA9* in both endothelial cells (ECs) and VSMCs; the primary resident cell types of the blood vessel wall. Each gene was expressed in both cell types with *SVEP1* (SF. 1A) and *ITGA4* (SF. 1B) more highly expressed in VSMCs and *ITGA9* expression higher in ECs (SF. 1C). Subsequent protein analysis revealed expression of SVEP1, integrin α4β1 and integrin α9β1 within the arterial wall, with all three proteins localised to VSMCs within the media layer of the arterial wall (Fig. 2A, 1-3, & SF.2). Immunofluorescent dual staining showed co-localization of SVEP1 with integrin α4β1 (Fig. 2B, 1-3) and integrin α9β1 (Fig. 2B, 4-6) in mouse aorta, and isolated human VSMCs (Fig. 2C, 1-3 & 4-6 respectively). SVEP1 protein was found to co-localise to both integrin α4β1 and integrin α9β1 at low levels in isolated HUVEC cells (SF.3). Relevant staining controls are shown in SF4.

Development of a human VSMC *in vitro* platforms for SVEP1 vasoconstrictive investigations

A limiting factor in smooth muscle contraction experiments is the loss of membrane channels and GPCRs within days of culturing following tissue extraction[25-27]. To overcome this issue, we developed a human iPSC-derived vascular smooth muscle cells (iVSMC) model with iPSCs differentiated into a mesodermal phenotype as a monolayer prior to differentiation into specialised VSMC phenotype[28]. iPSC pluripotency gene expression is stopped by day 4 (SF. 5B, 1&5). Cells differentiate into primitive streak cells (days 2-4, SF. 5B, 2&6) and mesodermal progenitors (days 3-6, SF. 5B, 3), with 94% of cells $CD140^+$ at day 8 (SF. 5B, 7). After a further 12 days culture in TGFβ and PDGF supplemented media, the iVSMCs express a panel of smooth muscle contractile markers (SF. 5C), reliably physically contract a collagen gel (SF. 5D, 1), and display an increase in $[Ca^{2+}]_i$ in response to a panel of GPCR vasoconstrictors (SF.5D, 2) compared to the limited contractile responses seen in cultured primary human VSMCs (SF. 5D, 3).

To interrogate the role of SVEP1 integrin α4β1 and α9β1 in VSMC contraction we used 2 complimentary methods. Gene expression of*SVEP1* , *ITGA9* and *ITGA4* were knocked down using siRNA in differentiated iVSMCs. We achieved a knockdown efficiency between 60-90% at the RNA level, with protein knockdown confirmed for integrin α4 and α9 by western blotting and immunofluorescence, and SVEP1 by immunofluorescence alone (SF. 6). We were unable to detect a reliable band of the correct molecular weight to reliably quantify SVEP1 protein expression. In addition to siRNA depletion of *SVEP1* , we generated$SVEP1^{-/-}$ knockout iPSCs using CRISPR-Cas9 which contain a 1 base pair deletion at position 130 in the coding sequence within exon 1 of *SVEP1* (SF.7). This isogenic pair of iPSCs were then differentiated into iVSMCs and used in calcium release experiments.

Σ″ΕΠ1 ανδ ιντεγριν α4 ορ α9 δεφιχιενχψ ενηανχες ″ΣΜ″ $[\ddot{\alpha}^{2+}]_\iota$ ρελεασε

SVEP1 siRNA treated isolated iVSMCs showed significant increases in Ca^{2+} release to a panel of vasoconstrictors that signal via different GPCRs including endothelin (ET)-1 (Fig. 3A,P <0.05), or carbachol (Fig. 3B,P <0.001) compared to non-targeted control (NTC) siRNA transfected cells. This effect was confirmed in$SVEP1^{-/-}$ iVSMCs where maximal calcium release to ET-1 (SF. 8A, P <0.01) and carbachol (SF. 8B,P <0.05), were also significantly enhanced compared to isotype control iVSMCs. Inhibition of either integrin α4β1 or α9β1 using siRNA caused enhanced iVSMC Ca^{2+} release to ET-1 (Fig. 4A, P <0.01 & P <0.05 respectively), whilst simultaneous inhibition of integrin α4β1 and α9β1 did not cause additional Ca^{2+} release (Fig. 4A,P <0.001). Similarly, *SVEP1* deficiency and blocking either integrin α4β1 (SF. 9A, P <0.05), integrin α9β1 (SF. 9B P <0.001), or integrin α4β1 and α9β1 dual inhibition using siRNA (Fig. 4B, P <0.05) or the dual integrin α4β1/α9β1 inhibitor BOP[29] (Fig. 4C,P <0.05) did not cause additional ET-1-mediated Ca^{2+} release compared to cells treated with*SVEP1* siRNA alone. Similar results were seen in iVSMCs stimulated with carbachol (SF. 9E P <0.05) and was confirmed in ET-1-stimulated $SVEP1^{-/-}$ iVSMCs treated with BOP (SF. 9D, P <0.05). These data show that SVEP1 reduces iVSMC Ca^{2+} release to several $G_{\alpha\chi/11}$

agonists via integrin α4β1 and α9β1.

Σ″ΕΠ1-ιντεγριν α4/9 σιγναλλινγ ινηιβιτς ωηολε εσσελ ςοντραςτιον

Perinatal mortality is observed in *Svep1* null mice, with mice displaying edema at E18.5[14].*Svep1* $^{+/-}$ mice, which are viable with no gross phenotypic effects[14,24] were therefore used for*ex vivo* analysis of vessel contraction.

Aortic vessel contraction was measured in response to several vasoconstrictors, with the thromboxane-A_2 agonist U46619 providing the most reliable response (SF.10A-D), which was then used in subsequent experiments. Vessels from *Svep1*$^{+/-}$ mice showed a significantly higher contraction to U46619 (Fig. 5A, 1.23 mN/mm^2, P <0.001, concentration independent) and PE (SF. 10E, 0.31 mN/mm^2,P <0.0001, concentration independent), compared to littermate controls. Incubation of vessels from C57BL/6J mice with an integrin α4 blocking antibody (10 μg/ml MCA1230Ga, Fig. 5B), or an integrin α9 blocking antibody (10 μg/ml 55A2C, Fig. 5C) significantly enhanced contraction to U46619 (ITGA4: 0.72 mN/mm^2,P =0.015, concentration independent. ITGA9: 1.45 (25 μg/ml) to 1.7 (100 μg/ml) mN/mm^2, P <0.0001, concentration dependent). Simultaneous blocking of integrin α4β1 and α9β1 using blocking antibodies (Fig. 5D) or BOP (3 μM, Fig. 5E) caused significant increase in vessel tension (Blocking antibodies: 1.09 mN/mm^2, P <0.0001, concentration independent. BOP: 1.53 (25 μg/ml) to 1.98 (100 μg/ml) mN/mm^2, all P <0.0001, concentration dependent), but did not enhance contraction compared to inhibition of individual integrins in isolation. Inhibition of integrin α4β1 and α9β1 using BOP did not enhance contraction in*Svep1*$^{+/-}$ mice (P =0.85, Fig. 5F).

″Γ″″ς ανδ ΠΚ″ ρεγυλατε Σ″ΕΠ1-ιντεγριν α4/9 ινηιβιτιον οφ σμοοτη μυσςλε ςοντραςτιον

Increases in intracellular Ca^{2+} occur through Ca^{2+} release from the sarcoplasmic reticulum and via an influx of extracellular Ca^{2+} through VGCCs[29]. Aortas from C57BL/6J were either pre-incubated with BOP (Fig. 6A) or integrin α4 and α9 blocking antibodies (SF.10F) in the presence or absence of the VGCC inhibitor nifidepine (1 μM) prior to U46619 stimulation. VGCC inhibition significantly lowered both normal U46619-mediated vessel contraction (NS vs. NF, 0.75 (25 μg/ml) to 1.43 (100 μg/ml) mN/mm^2,P <0.0001, concentration dependent, Fig. 6A), and the enhanced contraction caused by integrin α4/9 inhibition using BOP (BOP vs. BOP+NF, 1.05 (1 μg/ml) to 4.33 (100 μg/ml) mN/mm^2,P <0.0001, concentration dependent, Fig. 6A). In *Svep1*$^{+/-}$mice, inhibition of VGCCs also significantly reduced U46619-mediated contraction (Fig. 6B, 2.52 (25 μg/ml) to 6.76 (100 μg/ml) mN/mm^2, P <0.0001, concentration dependent). VGCCs activity is regulated by protein kinase C (PKC)[30]. Inhibition of PKC using bisindolylmaleimide I (BIM) (I), 10 μM) significantly reduced normal U46619-mediated contraction (NS vs. BIM (I), 1.96 (25 μg/ml) to 2.97 (100 μg/ml) mN/mm^2, P <0.0001, concentration dependent, Fig. 6C), the enhanced contraction caused by integrin α4/9 inhibition (BOP vs. BOP+BIM (I), 4.57 (25 μg/ml) to 5.18 (100 μg/ml) mN/mm^2, P <0.0001, concentration dependent, Fig. 6C). BIM (I) inhibition of PKC also significantly reduced U46619-mediated contraction in *Svep1*$^{+/-}$mice (Fig. 6D, 2.43 (25 μg/ml) to 5.98 (100 μg/ml) mN/mm^2, P <0.0001, concentration dependent). These results show that SVEP1 regulation of GPCR-mediated contraction occurs through regulating PKC-mediated VGCC Ca^{2+} influx into the vessel.

Discussion

The data presented here is the first to investigate the role of SVEP1 and integrin α9β1 in vasoconstriction. SVEP1 was found to bind to integrin α9β1 and for the first time, the closely related integrin α4β1. Cell adhesion studies suggest that SVEP1 binds to integrin α4β1 through its CCP21 domain. Within the vasculature and in isolated VSMCs, we found expression of SVEP1, integrin α4β1, and α9β1 to be predominantly localised within the media layer confirming previous data[23]. Reduction in *SVEP1* levels led to an increase in Ca^{2+} release in response to a panel of vasoconstrictors in iVSMC. Similar maximal increases in Ca^{2+} levels were seen upon inhibition of integrin α4β1 or α9β1, however, no additional alterations in Ca^{2+}release were seen upon co-inhibition of SVEP1 and the integrins. Comparable results were detected in whole vessel contraction with*Svep1*$^{+/-}$ aortic rings displaying enhanced contraction compared to aortas from litter-mate controls, whilst inhibition of integrin α4β1 or α9β1 also enhanced contraction. As seen in isolated cells, no

additional contraction was seen when both SVEP1 and integrin α4β1 or α9β1 were simultaneously inhibited, suggesting a level of redundancy or a ceiling effect of SVEP1 regulation upon vessel contraction.

While no vasoregulatory role has previously been described for SVEP1, a comparable study within the airway found ligation of integrin α9β1 to prevent airway hyperresponsivness[8], a phenotype similar to the role of SVEP1 reducing vascular hyperresponsivness presented here. While the role of SVEP1 was not specifically investigated in the airway study, GTEx and the Human Protein Atlas describe SVEP1 expression in the lung, oesophagus and intestine, providing the possibility that SVEP1 has a similar role in reducing smooth muscle hyper-contractility in several tissues.

Our studies showed PKC-mediated influx of Ca^{2+} via VGCCs to be the dominant mechanism in U46619-mediated vessel contraction. U46619 caused the most reliable aortic vessel contractions in studies, however, the signalling mechanisms downstream of the receptor are varied across smooth muscle tissue types: In the intrarenal artery, the mechanism is VGCC dependent, and partially PKC dependent[31] as seen within our aortic model. Within the bovine pulmonary artery contraction does not require VGCCs[32], whilst in the rat mesenteric artery[33] and the rat caudal artery[34]PKC is not required, suggesting a diverse downstream signalling mechanism across tissues. Our own studies demonstrate the importance of a PKC-dependent VGCCs signalling mechanism in aortic smooth muscle (Fig. 7). There is evidence that other GPCRs can activate integrins via PKC-dependent "inside-out signalling"[35,36], with PKC activity upstream of integrins the activated integrin inducing tyrosine phosphorylation of focal adhesion-associated proteins[35-37]. Studies into VSMC contraction initiated by direct integrin ligation also indicated a dominant role for VGCCs. Whole-cell recordings from arteriolar myocytes show αvβ3 to inhibit VGCC current[3,5]. Integrin α4β1 and α5β1 ligation enhances L-type Ca^{2+} current [4-7], and integrin α7β1 regulates both transient elevation of $[Ca^{2+}]_i$ from IP_3evoked Ca^{2+} release from intracellular stores and extracellular Ca^{2+} influx through VGCC in skeletal muscle[38]. These described studies administer synthetic peptides such as RGD or LDV to mimic important vasoactive ECM fragments, termed matrikines, which are otherwise un-exposed within the full-length ECM molecules[39-41]. Dysregulation of the ECM is linked to several vascular-associated diseases including CAD[42-44], heart failure[45], and stroke[46]. SVEP1 is known to be targeted by the protease ADAMTS-7 [47] which is linked to atherosclerotic plaque formation[48-50], and contains the linear peptide sequences RGD (which binds to integrin αv proteins) and LDV sequences (which bind to integrin α4 and α9)[51-53]. It would be interesting to determine whether SVEP1 breakdown products had altered vasoregulatory effects compared to full length SVEP1.

Our data identifies SVEP1 and integrins α4β1 and α9β1 as new mediators of GPCR-mediated vasoconstriction. Notably, human genetic studies have identified associations between variants in both SVEP1 and integrin α9β1 and BP. Our data provide a possible explanation for both associations and warrants further investigation. Future studies should investigate whether similar contractile profiles are seen within resistance arteries and whether these effects contribute to an altered BP and if this is affected by the BP-associated variants.

In conclusion we have described for the first time how the ECM protein SVEP1 prevents VSMC hyper-contractility via integrin α4β1 and/or α9β1 by reducing Ca^{2+} influx through VGCCs, providing a new link between a novel ECM protein and VSMC contraction.

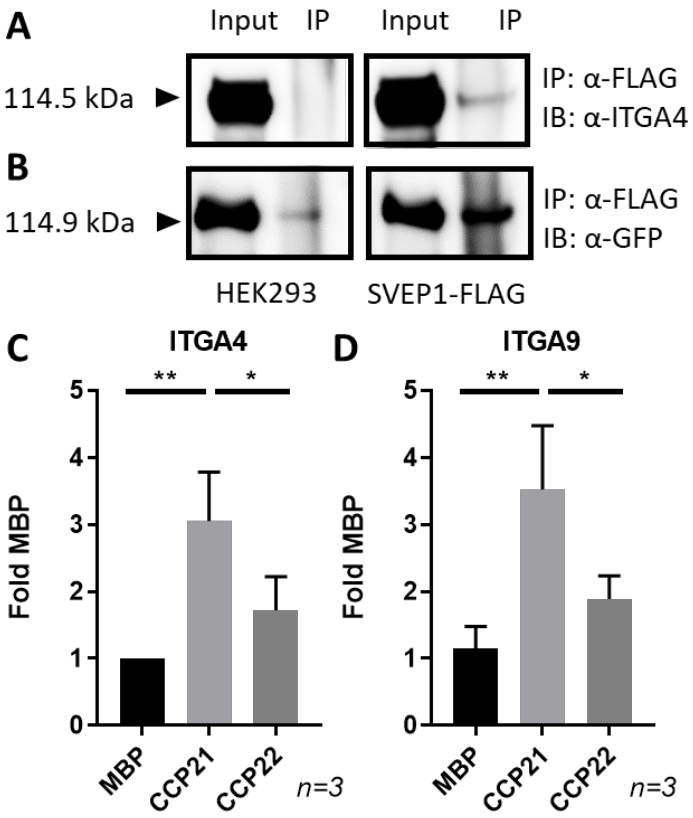

Figure 1: ITGA9 and ITGA4 bind to SVEP1

Recombinant SVEP1 with a C-terminal FLAG tag were transfected into HEK293 cells. Cells were then transfected with recombinant ITGA4 or recombinant ITGA9, with ITGA9 containing an additional N-terminal GFP-tag, and then pulled down with an anti-FLAG mAb-conjugate. The precipitates were subjected to a 4-12% SDS-PAGE under reducing conditions and visualised by immunoblotting with anti-ITGA4 (A), or anti-GFP (B). Binding efficiency of HEK293 cells transfected with ITGA4 (C) or ITGA9 (D) to surface coated with 100 nM manose binding protein (MBP), CCP21 or CCP22 (n=3, * P<0.05, ** P<0.01, one-way ANOVA, Tukey's post-test).

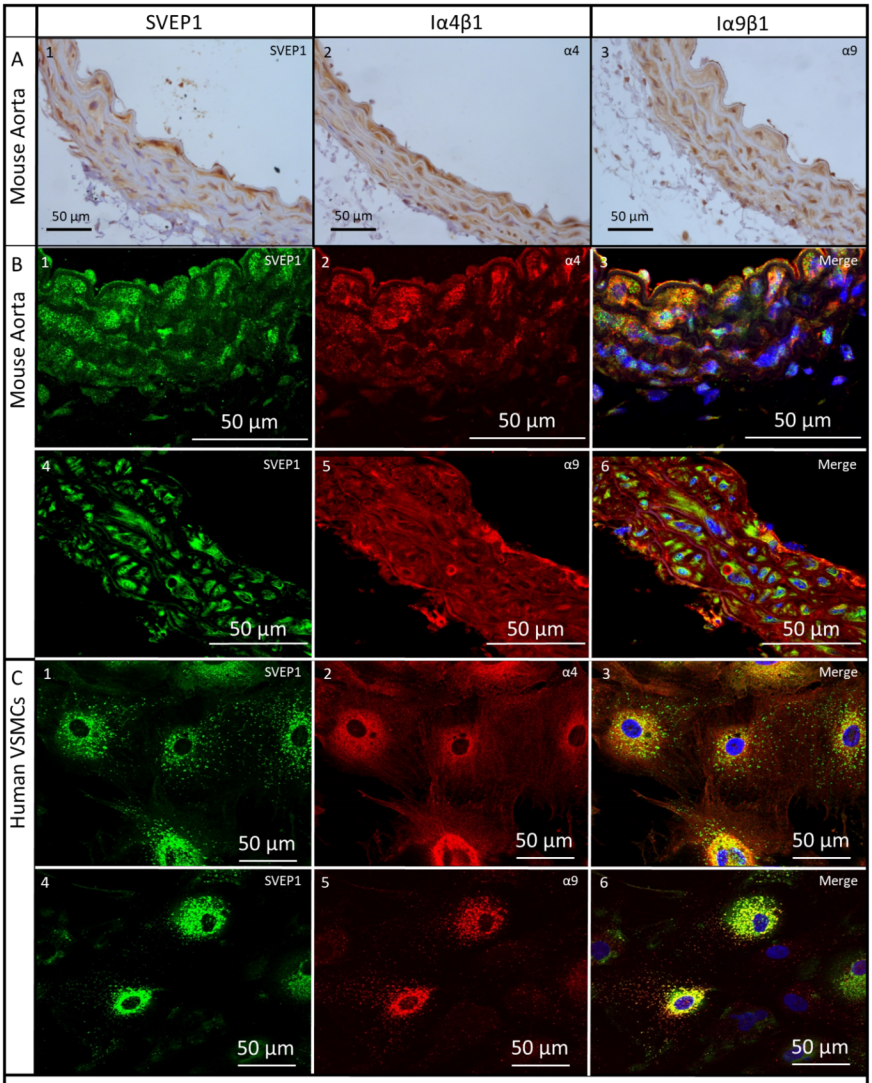

Fig 2: SVEP1, Iα4β1 and Iα9β1 in vascular smooth muscle.
A: Immunohistochemical staining of SVEP1 (1), integrin α4β1 (2), and integrin α9β1 (3) in mouse aorta sections. B: Dual fluorescent staining of SVEP1 (1 & 3) and integrin α4β1 (2 & 3), and SVEP1 (4 & 6) and integrin α9β1 (5 & 6) in mouse aorta sections. C: Dual fluorescent staining of SVEP1 (1 & 3) and integrin α4β1 (2 & 3), and SVEP1 (4 & 6) and integrin α9β1 (3 & 4) in human vascular smooth muscle cells.

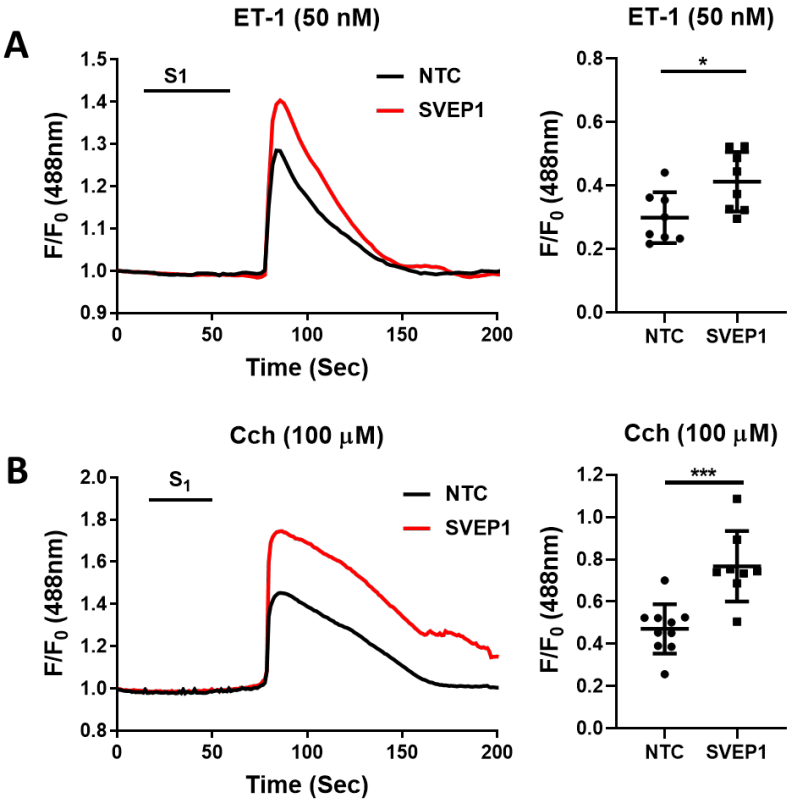

Figure 3: SVEP1 inhibition enhances iSMC contraction to ET-1 or carbachol.

iSMCs were treated with either non-targeting control (NTC), or SVEP1 siRNA for 48 hrs prior to Fluo3 loading and vasoconstrictior challenge for 45 seconds. (A) Mean trace and maximal fluorescence signal (dot plot) are shown for ET-1 (50 nM), and Cch (100 μM) (B) (±SD, n=5-10 independent experiments each comprising 56-225 cells, * P<0.05, *** P<0.001).

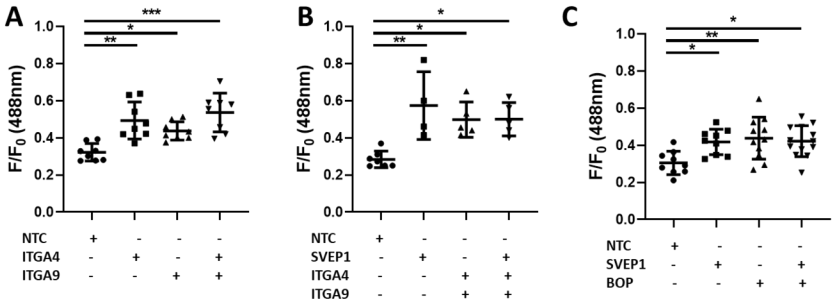

Figure 4: Simultaneous inhibition of SVEP1 and integrin α4 or α9 does not induce additional vasocontraction
iSMCs were treated with non-targeting control (NTC), ITGA4, ITGA9 or SVEP1 siRNA for 48 hrs, or the dual integrin α4β1-α9β1 inhibitor BOP for 2 hours prior to Fluo3 loading and ET-1 (50 nM) challenge for 45 seconds. Maximal fluorescence signal (F/F_0) are shown (±SD, n=4-13 independent experiments each comprising 20-200 cells, One-way ANOVA, Tukey's post-test: * P<0.05, ** P<0.01, ***P<0.001).

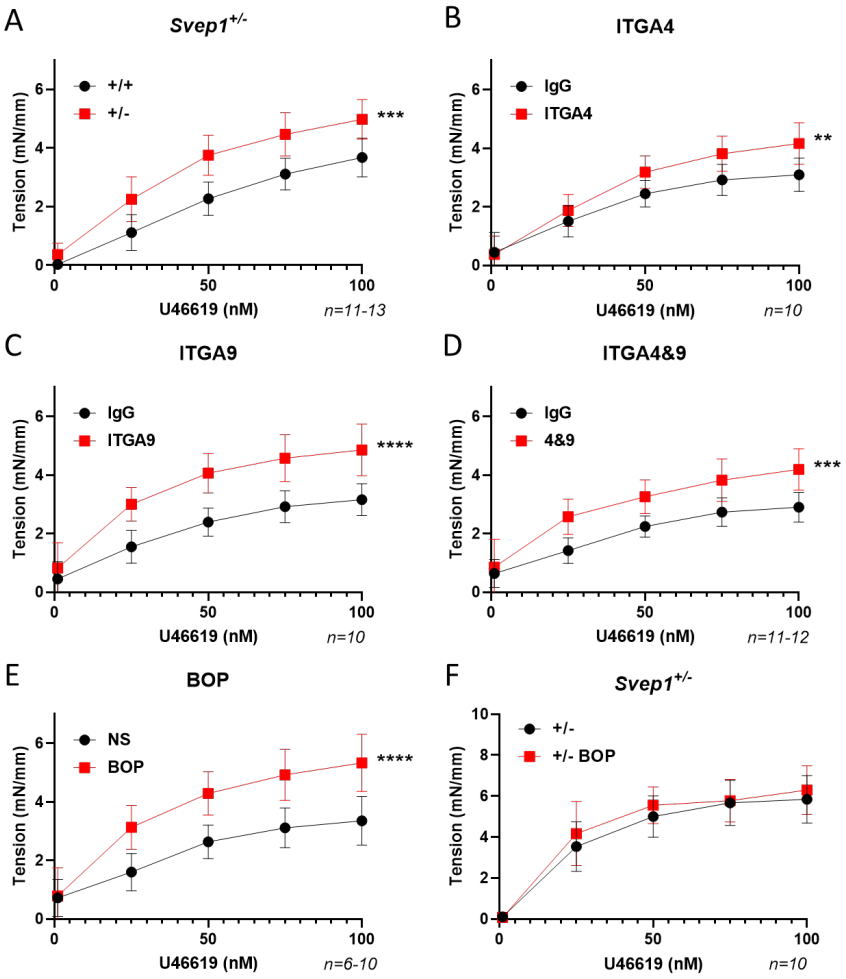

Figure 5. SVEP1 or integrin α4/9 inhibition enhances blood vessel contraction
Aortas from *Svep1*$^{+/-}$ mice were stimulated with U46619 (A) and force generation was recorded by wire myography. Aortas from C57BL/6J mice were incubated overnight with an integrin α4 (10 µg/ml) (B), integrin α9 (10 µg/ml) (C), a combination of both integrin α4 & α9 blocking antibodies (D), or the dual integrin α4 and α9 inhibitor BOP (3 µM) (E) prior to U46619 application. Aortas from *Svep1*$^{+/-}$ mice were incubated overnight with BOP (F) and force generation was recorded (point estimates are mean values; bar represents 95% confidence intervals; *p*-values derived from mixed-effect models, ** P<0.01, *** P<0.001, **** P<0.0001).

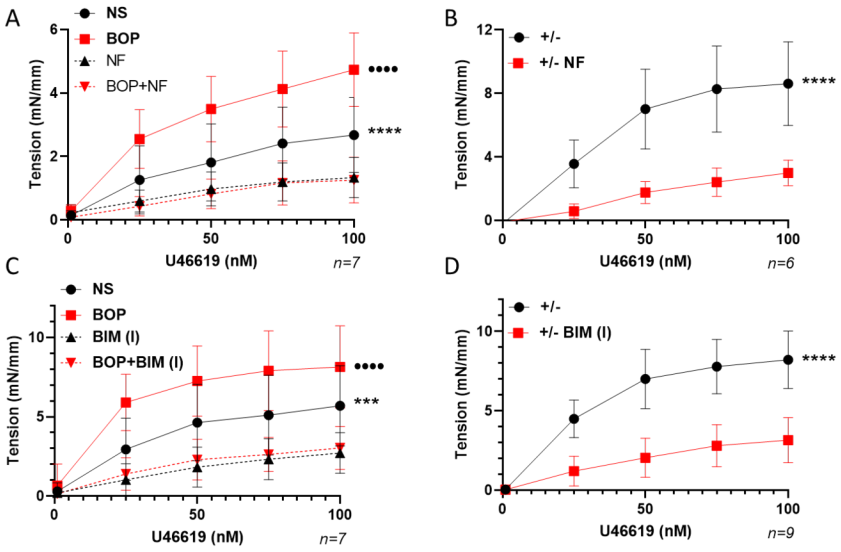

Figure 6: Integrin α4/9 regulates blood vessel contraction via Ca^{2+} influx through VGCCs in a PKC dependent manner

Aortas from C57BL/6J mice were incubated with the dual integrin α4/9 inhibitor BOP overnight and incubated with the VGCC blocker nifidepine (NF) prior to U46619 application and force generation was recorded (A, point estimates are mean values; bar represents 95% confidence intervals; *p*-values derived from mixed-effect models, **** $P<0.0001$ NS vs. NF, •••• $P<0.0001$ BOP vs. NF). Aortas from *Svep1*$^{+/-}$ mice were incubated with with NF (B, **** $P<0.0001$). Aortas from C57BL/6J mice were incubated BOP overnight and incubated with the PKC inhibitor BIM (I) (C, *** $P<0.001$, NS vs. BIM (I), •••• $P<0.0001$ BOP vs. BIM (I)). Aortas from *Svep1*$^{+/-}$ mice were incubated with BIM (I) (D, **** $P<0.0001$).

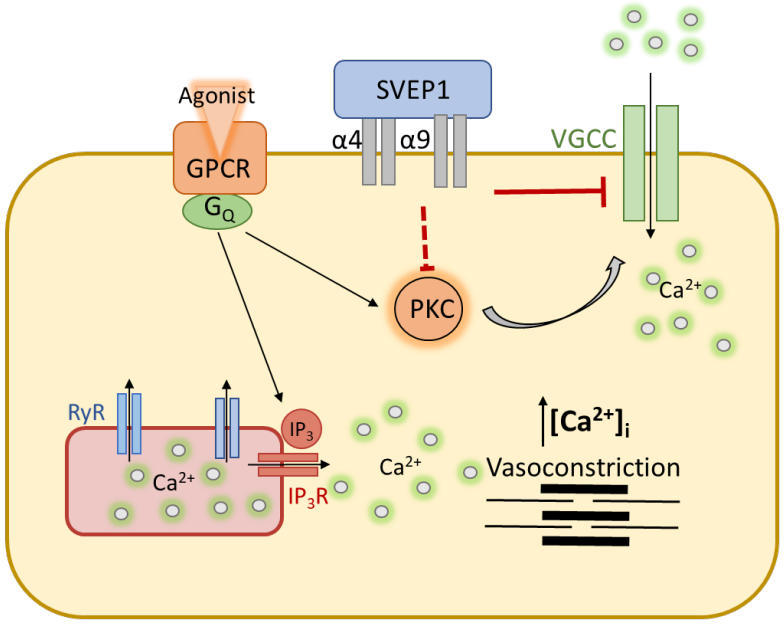

Figure 7: Schematic of how SVEP1 regulates GPCR-mediated vasoconstriction

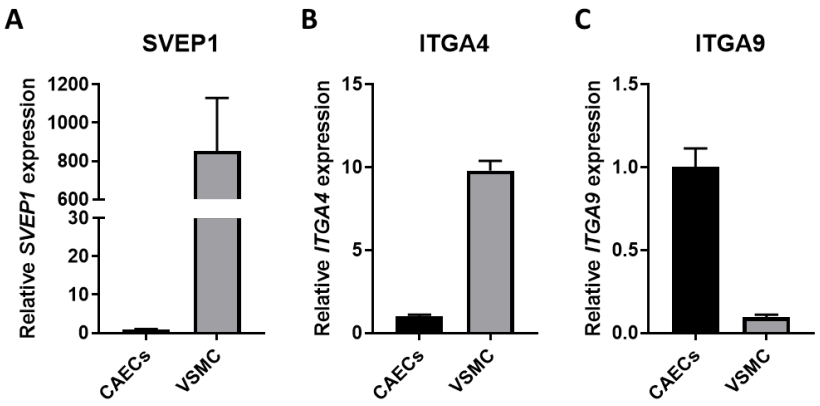

Supplemental Figure 1: SVEP1 and integrin expression in the vasculature

SVEP1, ITGA4 and *ITGA9* mRNA expression was measured using qRT-PCR in human coronary artery endothelial cells (CAEC) and vascular smooth muscle cells (VSMC). Results are normalised relative to *SVEP1* gene expression in CAEC (±SD n=3).

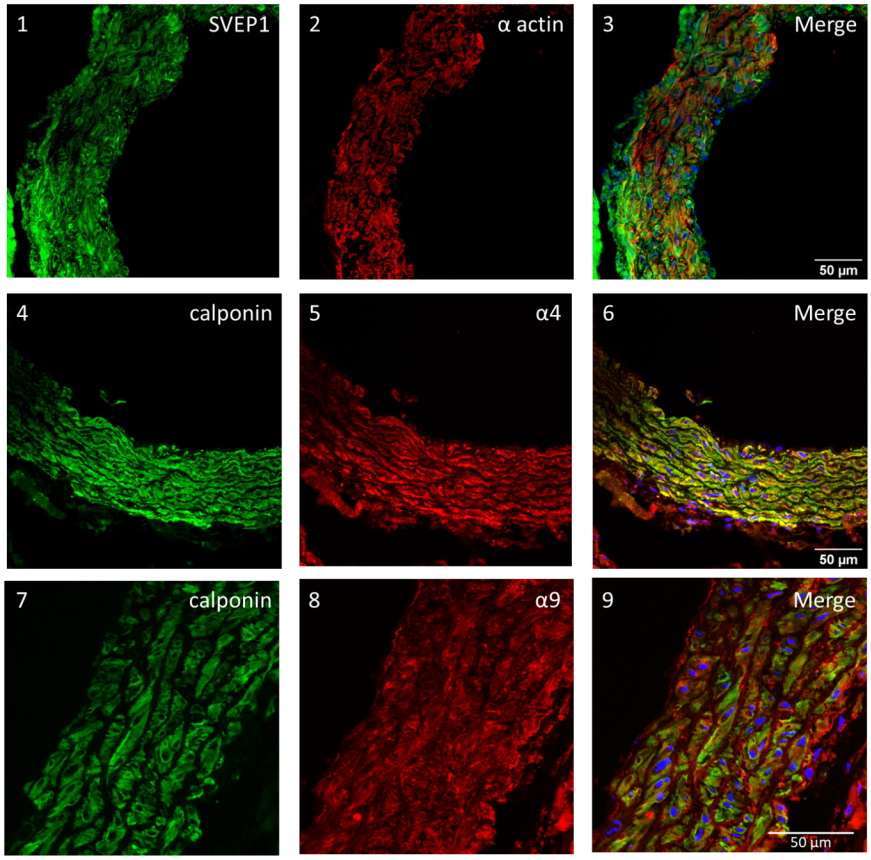

Supplemental Figure 2. SVEP1, Iα4β1 and Iα9β1 are localised to smooth muscle cell layer

Dual fluorescent staining of SVEP1 and smooth muscle α-actin (1-3), integrin α4β1 and calponin (4-6), and integrin α9β1 and calponin (7-9) in mouse aorta sections.

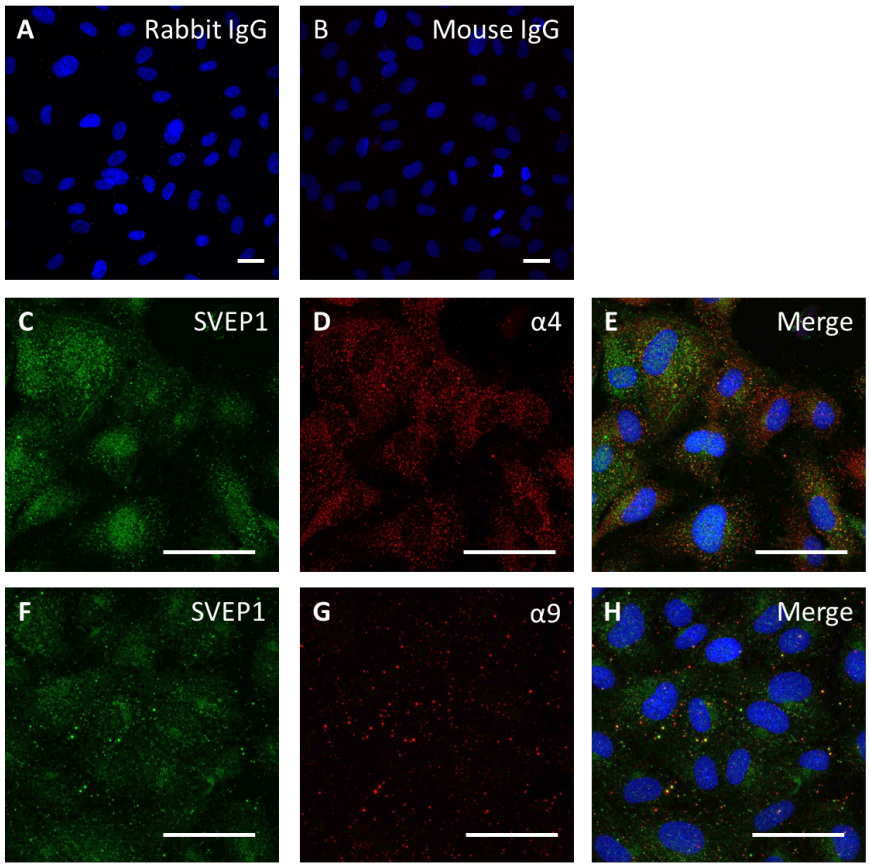

Supplemental Figure 3: SVEP1, integrin α4β1 and α9β1 are expressed on endothelial cells

HUVECs were fixed and stained with 3 $\mu g ml^{-1}$ rabbit IgG (A), or 2 $\mu g\ ml^{-1}$ mouse IgG (B) and appropriate secondary antibody. Dual fluorescent staining of SVEP1 (C & E) and integrin α4β1 (D & E), and SVEP1 (F & H) and integrin α9β1 (G & H). Scale bar indicates 50 µm.

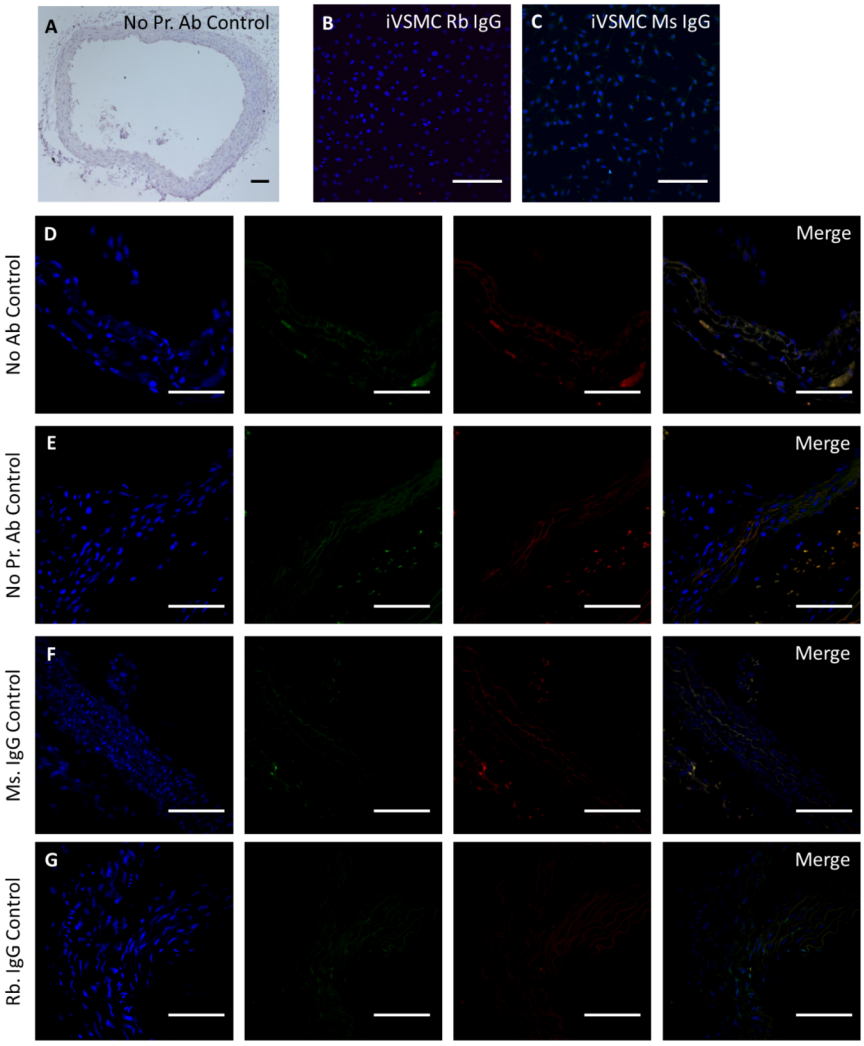

Supplemental Figure 4: Antibody controls for ICC staining
Aortic section stained for IHC had no primary antibodies added (A). iVSMCs were stained with 3 $\mu g ml^{-1}$ rabbit IgG (B), or 2 $\mu g\ ml^{-1}$ mouse IgG (C) and appropriate secondary antibody. Aortic sections were imaged on a confocal microscope using the same laser settings as used for staining. Sections had no antibodies added (D), no primary antibodies (E), Mouse IgG at 2 $\mu g\ ml^{-1}$ (F) or rabbit IgG at 3 $\mu g ml^{-1}$ (G). Scale bar indicates 100 µm.

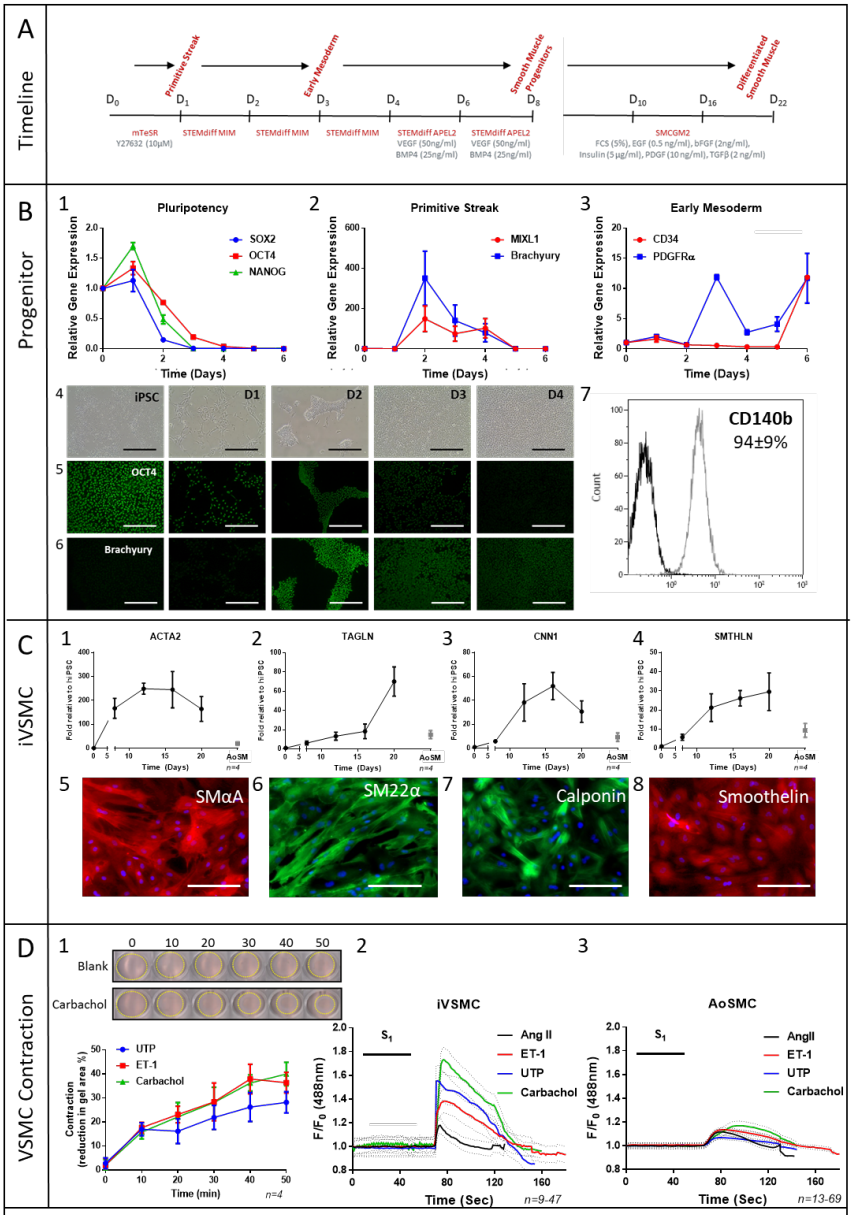

Supplemental Figure 5: iPSC differentiation into iVSMC protocol

A) Timeline of iPSC differentiation into iVSMCs including the flow cytometric analysis of CD140^{+} cells at day 8. **B**) qPCR data showing pluripotency (1), primitive streak (2) and mesodermal gene expression (3) (mean±SEM, n=4). **C**) iVSMC progenitor cells were cultured in media supplemented with PDGF-BB (10 ng/ml) and TGFβ (2 ng/ml) for 12 days before characterisation. qPCR expression of ACTA2 (1), CNN1 (2), and SMTHLN (3) (mean±SEM, n=4), and protein expression data of smooth muscle α actin (4), calponin (5) and smoothelin (6), scale bar indicates 100 μm. **D**) iVSMC contractility was measured by collagen gel contraction (1) and intracellular Ca^{2+} release (2) to several vasoconstrictors. Relative contractility of cultured human aortic smooth muscle cells (AoSMC) to the same vasoconstrictors is shown in (3).

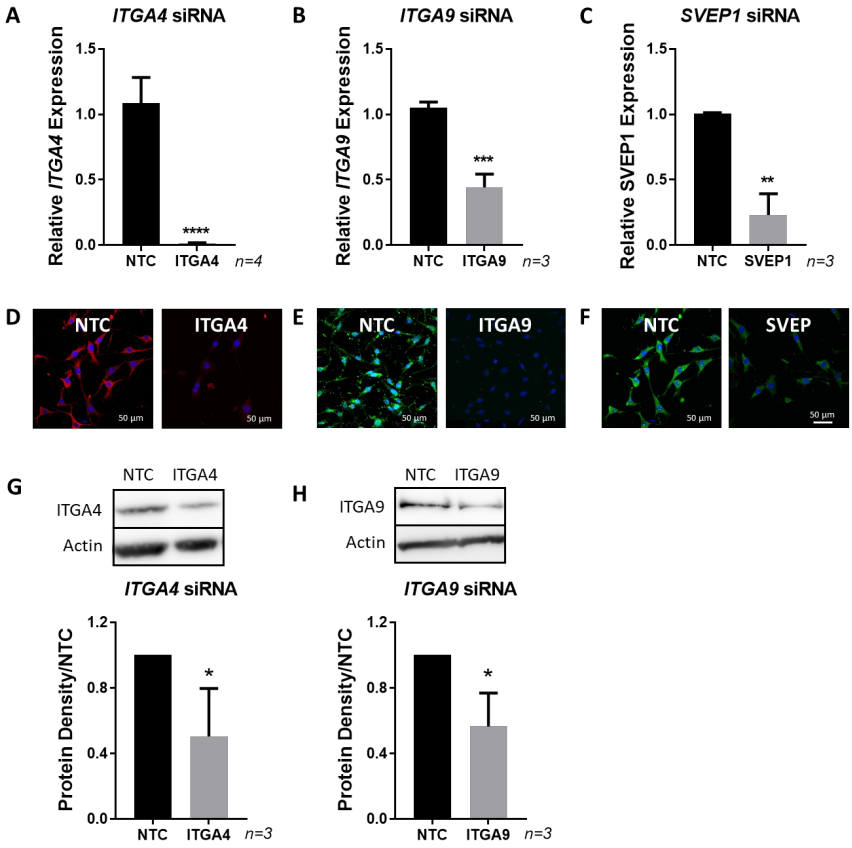

Supplemental Figure 6: Quantification of ITGA4, ITGA9 and SVEP1 siRNA degradation

iSMCs were transfected with 100 nM of non-targeting control (NTC), ITGA4, ITGA9, or SVEP1 siRNA for 48 hours. Cells were lysed and relative gene expression of *ITGA4* (A), *ITGA9* (B), and *SVEP1* (C) were measured by quantitative PCR (***p*>0.01, ****p*>0.001, *****p*>0.0001, unpaired t-test) . Cells were fixed and ITGA4 (D), ITGA9 (E), and SVEP1 (F) protein expression was visualised by immunocytochemistry. Cells were also lysed and ITGA4 (G), and ITGA9 (H) protein expression was quantified by densitometry (**p*>0.05, ***p*>0.01, unpaired t-test). We were unable to confirm a reliable SVEP1 protein band and so excluded this from our study.

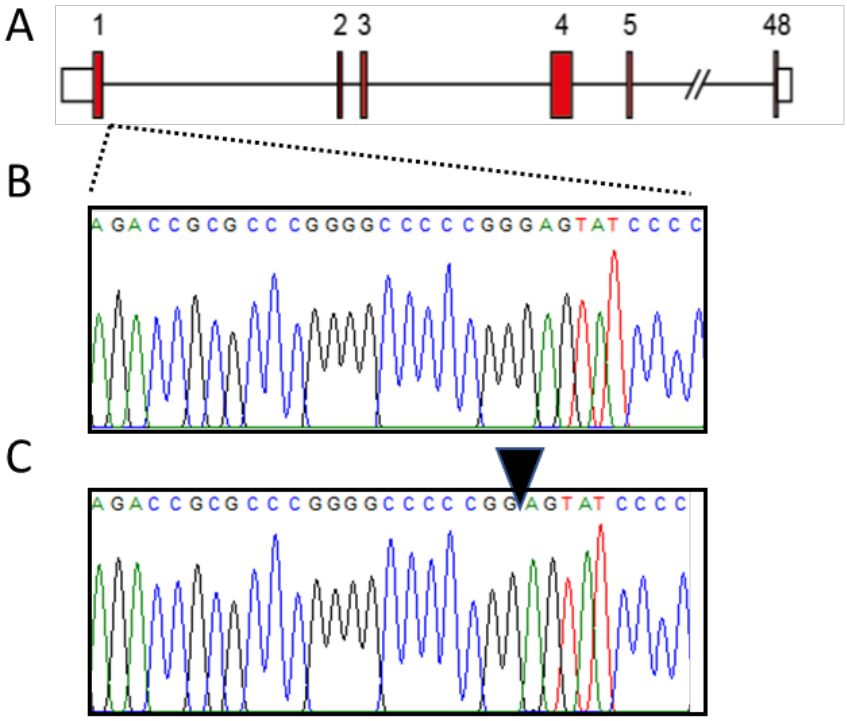

Supplemental Figure 7. Generation of *SVEP1* knockout iPSCs.

(A) Truncated schematic of *SVEP1* gene structure. CRISPR guide RNA targeted region in exon 1 of *SVEP1. (B) SVEP1* sequencing from parental iPSC line. (C) *SVEP1* exon 1 sequencing from SVEP1$^{-/-}$ iPSC line with deletion event shown by the black triangle.

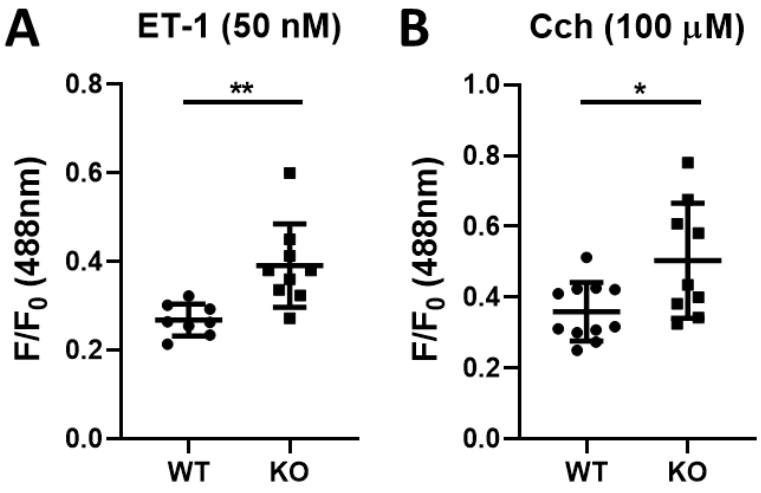

Supplemental Figure 8: SVEP1$^{-/-}$ iSMCs exhibit enhanced contraction to ET-1 or carbachol.

iVSMCs differentiated from parental wild type (WT) isotype control iPSCs or *SVEP1*$^{-/-}$ KO iPSCs were loaded with Fluo3 prior to vasoconstrictior challenge for 45 seconds. Maximal fluorescence signal (F/F_0) are shown for ET-1 (50 nM) (A), or Cch (100 μM) (B) (±SD, n=8-13 independent experiments each comprising 48-113 cells, * P<0.05, ** P<0.01)

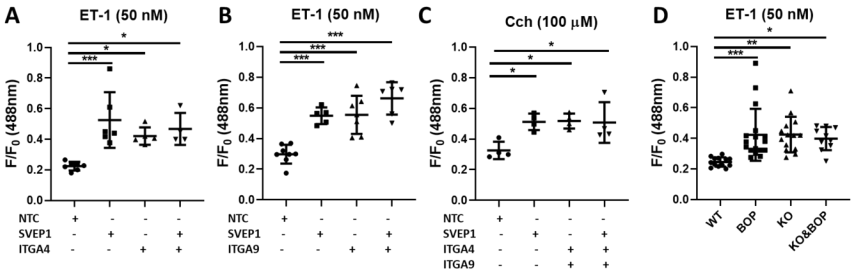

Supplemental Figure 9: Simultaneous inhibition of SVEP1 and integrin α4 or α9 does not enhance contraction to a panel of vasoconstrictors

iVSMCs were treated with non-targeting control (NTC), ITGA4, and SVEP1 siRNA (A), NTC, ITGA9 and SVEP1 siRNA (B) for 48 hrs prior to Fluo3 loading and ET-1 (50 nM) challenge for 45 seconds. iVSMCs were treated with non-targeting control (NTC), ITGA4, ITGA9 and SVEP1 siRNA (C), for 48 hrs prior to Fluo3 loading and carbachol (100 μM) challenge for 45 seconds. Maximal fluorescence signal (F/F_0) are shown (±SD, n=4-5 independent experiments each comprising 8-59 cells, One-way ANOVA, Tukey's post-test: * P<0.05, ** P<0.01, *** P<0.001). (D) iVSMCs differentiated from parental wild type (WT) isotype control iPSCs or SVEP1 KO iPSCs were treated with the dual integrin α4β1-α9β1 inhibitor BOP for 2 hours prior to Fluo3 loading and ET-1 (50 nM) challenge for 45 seconds. Maximal fluorescence signal (F/F_0) are shown (±SD, n=5-17 independent experiments each comprising 109-148 cells, One-way ANOVA, Tukey's post-test: * P<0.05, ** P<0.01, *** P<0.001).

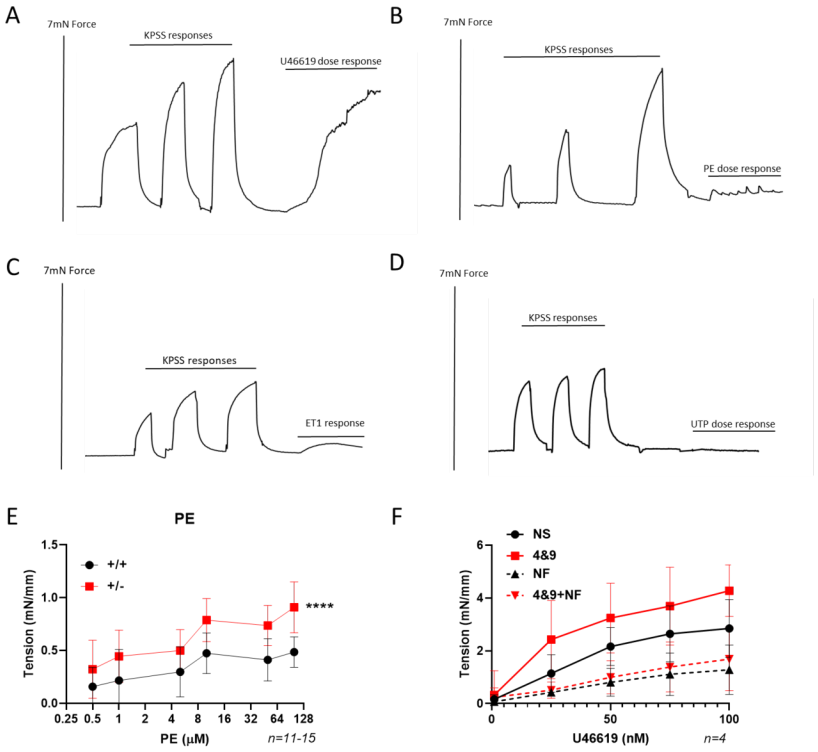

Supplemental Figure 10: Aortic contraction to a panel of vasoconstrictors.

Example traces showing force generation of aortas from C57BL/6J mice were stimulated with U46619 (A), phenylephrine (PE, B), ET-1 (C), or UTP (D). Aortas from *Svep1*$^{+/-}$ mice or littermate controls were stimulated with PE and force generation was recorded by wire myography (E, point estimates are mean values; bar represents 95% confidence intervals; *p*-values derived from mixed-effect models, **** P<0.0001). Aortas from C57BL/6J mice were pre-incubated with integrin α4 and α9 blocking antibodies overnight and incubated with the VGCC blocker nifidepine (NF) for 30 minutes prior to U46619 application (F, mean±95% CI).

Methods

Cell culture

All cell lines were maintained at 37 °C in a 5% CO_2incubator. HEK293 wild type cells were maintained in DMEM supplemented with 10% (*v/v*) foetal calf serum (FCS) and integrin α4 over-expressing cells were maintained in DMEM supplemented with 10% (*v/v*) FCS and 500 μg mL^{-1} geneticin.

Human induced pluripotent stem cells (iPSCs) (Cell line GM23720, NIGMS collection from the Coriell institute for medical research) were maintained on growth factor reduced (GFR) matrigel-coated plates in mTeSR Plus media (STEMCELL Technologies). Cells were passaged using ReLeSR (STEMCELL Technologies) and re-plated as small clumps of cells at a dilution of 1:10 to 1:20. For SMC differentiation, iPSCs were dissociated with Accutase and plated on GFR Matrigel at a density of $2.5x10^4$ cells cm^{-2} in ROCK inhibitor (Y-27632, 10 μM)-supplemented mTeSR Plus media for 24 hours. Media was replaced with STEMdiff MIM (STEMCELL Technologies) for 72 hours, with media replaced every 24 hours. After 72 hours, the MIM was replaced with SMC Induction medium consisting of STEMdiff APEL-2 medium (STEMCELL Technologies) supplemented with 50 ng ml^{-1} VEGF and 25 ng ml^{-1} BMP4 for 4 days, with media replaced after 2 days. On day 8, cells were dissociated using Accutase and plated on collagen IV (30 μg ml^{-1} coated wells) in Smooth Muscle Cell Growth Medium 2 (SMGM2 (Promocell) supplemented with 10 ng ml^{-1} PDGF-BB, 2 ng ml^{-1} TGFβ, 0.5 ng ml^{-1} EGF, 2 ng ml^{-1} bFGF, 5 μg/ml^{-1} insulin and 0.05 ml/ml FCS for a further 14 days. Experimentation was conducted on cells between day 32 and day 40.

Generation of SVEP1$^{-/-}$ iPSC lines

An isogenic pair of *SVEP1* GM23720 iPSC line was generated by CRISPR genome editing in collaboration with Horizon Discovery Ltd. A guide RNA targetting GAGACCGCGCCCGGGG*CCCCCGGGAGTATCCCCGCGCCG* CCCGCTCCTGGCGA, a region within exon 1 of Ensembl SVEP1 transcript SVEP1-003 (ENST00000374469.5) was designed. The underlined highlighted sequence indicates the protospacer adjacent motif and the italic sequence indicates the guide RNA. This guide RNA was co-transfected into iPSCs with a plasmid expressing CAS9. After transfection, iPSCs were serially diluted into 96 well plates to generate single cell clones. Single cell clones were genotyped by sequencing PCR products generated using primers CAGCCGCTCTGTCTCCAG and AGGAGATGGCAGGGATCTCT.

Cell transfection

iVSMCs were transiently transfected with non-targeting control (Qiagen siRNA, cat: 1022076), ITGA9 (Qiagen FlexiTube siRNA, cat: S100034272), SVEP1 (ThermoFisher Scientific Stealth siRNA, cat: 1299001) or ITGA4 (Dharmacon SMARTpool of 4 siRNAs, cat: SO-2757075G) using Lipofectamine RNAiMAX (Thermofisher) diluted in OptiMEM in SMGM2. Media was changed after 24 hours, with cells used at 48 hours.

Single-Cell Ca^{2+} iVSMC Imaging

iVSMCs were loaded with the Ca^{2+}-sensitive dye Fluo-3, AM (3 μmol/L 60 min) (Thermofisher). Cells were maintained at 37°C using a Peltier unit and continually perfused with Krebs-Henseleit buffer (mmol/L: 134 NaCl, 6 KCl, 1 $MgCl_2$, 1.2 KH_2PO_4, 10 glucose, 10 HEPES, 1.3 $CaCl_2$, pH 7.4). Real-time images were taken using an epifluorescence Nikon Eclipse TE200 microscope (Nikon) (×20 objective) and Volocity 6.1.1 image software (Quorum Technologies). Cells were stimulated with vasoconstrictors applied via the perfusion line for 45 seconds, and Fluo-3 emission was assessed at [?]520 nm. $[Ca^{2+}]_i$ changes are displayed as the fluorescence emission relative to basal fluorescence (F/F_0).

Svep1$^{+/-}$ Mouse Studies

Animal experimentation was approved by the local animal ethics committee and performed according to ARRIVE (Animal Research: Reporting of In Vivo Experiments) guidelines and under United Kingdom Home Office Project Licence (P4E9A1CCA). All mice were housed in a specific pathogen-free facility in an individually ventilated caging system. Mice were group housed wherever possible, and their health status was checked routinely. No mice demonstrated any adverse effects. C57BL/6J mice were purchased origi-

nally from Charles River, then bred in the Preclinical Research Facility in the University of Leicester, to provide animals for the study. Genetically altered animals, B6N(Cg)-*Svep1* $^{tm1b(EUCOMM)Hmgu}$/J (reporter-tagged deletion allele, https://www.informatics.jax.org/allele/MGI:5509058;*Svep1* $^{+/-}$) was purchased from the Jackson Laboratory (Bar Harbor, ME, USA). 8-24 week old mice of both genders were used in experiments.

Wire myography

Aortic rings where integrin α4 and/or α9 were inhibited were incubated with either BOP or blocking antibodies overnight at 37 °C in a 5% CO_2 incubator in DMEM basal media. Contractile force recordings were made from [?]2 mm ring segments of aortic rings mounted at 1.2 mN tension in a Mulvany-Halpern wire myograph (Danish Myo Technology). The bath solution contained (mmol/L): NaCl 136, KCl 5, $MgSO_4$ 1.2, $CaCl_2$ 1.8, glucose 5, mannitol 15, HEPES 10, NaH_2PO_4 0.5, Na_2HPO_4 0.5 pH 7.4. NaCl was reduced to 81 mmol/L and replaced with 60 mmol/L KCl for the high K^+ solution. Vessels were depolarised in high K^+ solution 3 times prior to initiation of contractile studies. Pharmacological inhibitors (nifidepine (3 μM), BIM (I) (10 μM), or BOP (3 μM) were added directly to the organ bath, maintained at 37°C, 30 minutes prior to addition of vasoconstrictors (U46619, PE, UTP, ET-1).

RNA extraction, cDNA synthesis and RT-PCR

Total RNA was extracted with RLT buffer and purified using an RNeasy mini kit (Qiagen®) according to manufacturer's instructions. RNA yield was determined using a NanoDrop ND-8000 spectrometer. Genomic DNA was removed by DNase I incubation using the RNase-Free DNase Set (Qiagen®) and RNA was converted to cDNA using SensiFAST cDNA synthesis kit (Geneflow). Quantitative PCR (qPCR) was completed using the SYBR® 3 Green master mix, with amplification carried out in triplicate using a Rotor-Gene® Q (Qiagen®). Expression of target genes were normalised to reference gene 36B4. Primer sequences are listed in Table S1.

Immunohistochemical (IHC) and immunofluorecence (IF) staining

Primary antibodies that were used for IHC and IF are listed in Table S2. Heat- induced antigen retrieval was performed with Antigen Unmasking Solution, Tris-Based (Vector, H-3301) for all antibodies. For IHC staining, endogenous peroxidase activity was blocked in 0.3% H_2O_2 in deionised water. Nonspecific binding was reduced by incubation in 2.5% goat serum. Sections were treated with mouse Ig blocking reagent (Vector, MKB-2213-1) before application of the primary mouse antibody. Rabbit primary antibody binding was detected with goat anti-rabbit ImmPRESS HRP goat anti-rabbit IgG (Vector, MP-741) and mouse primary antibody binding was detected with Mouse-on-Mouse ImmPRESS anti-mouse Ig reagent (Vector, MP-2400). Colour was developed with DAB-substrate chromogen system (Vector, SK-4100). Images were acquired with a DM2500 Leica microscope (Leica Microsystems).

For IF staining of aortic sections, rabbit primary antibody binding was detected with goat anti-rabbit IgG (Alexa Fluor-488), mouse primary antibody binding was detected with goat anti-mouse IgG (Alexa Fluor-647), and goat primary antibody was detected with donkey anti-goat IgG (Alexa Fluor-594). DAPI was used for nuclei visualization. Images were acquired using an Olympus FV1000 confocal laser scanning microscope with images analysed using Fiji[54].

iVSMCs or HUVECs were grown on μ-Slide 8 well chamber slides (Thistle Scientific) and fixed in 4% PFA. SVEP1, Integrin α4 and α9 staining was performed on non-permeabilised cells. For all other staining, cells were permeabilised in 0.5% Triton-X. Non-specific binding was reduced by incubation in 1% bovine serum albumin (BSA), 22.5 mg ml-1 glycine, 0.1% tween-20 PBS solution, with additional blocking in a 10% goat serum PBS solution. Cells were incubated overnight at 4°C in primary antibody (listed in Table S2) diluted in 10% goat serum. After washing, cells were incubated in 10% goat serum containing complementary secondary antibodies. Nuclei were visualised by DAPI counterstaining. Images were acquired using an Olympus FV1000 confocal laser scanning microscope with images analysed using Fiji.

Flow cytometry

iVSMCs were dissociated using Accutase. $CD140^{+}$staining was quantified using single cell suspensions incubated using an APC-direct labelled antibody diluted in flow buffer (BSA (0.5%), EDTA (2 mM), PBS, pH 7.2). Samples were run on a Beckman Coulter Gallios flow cytometer and analysed using Kaluza flow cytometry analysis software (Beckman Coulter).

Western blotting

Cells were lysed in modified RIPA buffer (Tris HCl (50 mM), EDTA (1 mM), Halt Protease Inhibitor cocktail (Thermofisher), pH7.4. Western Blot Analysis Protein content was measured using the Novex® protein separation kit (Thermofisher). Equal amounts of protein lysates were separated by SDS-PAGE before blotting onto nitrocellulose membrane. Membranes were probed with primary antibodies (see Table S2), detected with horseradish peroxidase conjugated secondary antibodies and visualised by enhanced chemiluminescence (GE Healthcare). Quantitative signals were derived by densiometric analysis using ImageQuant TL on an ImageQuant LAS 4000 Luminescent Image Analyzer (Fujifilm).

Immunoprecipitation

Constructs expressing ITGA9-GFP or ITGA4 were transfected into HEK293WT or HEK293 cells overexpressing SVEP1-FLAG. 48 hours post transfection the transfected cells were scraped into lysis buffer (mmol/L-1: 50 Tris-HCL, 150 NaCl, 1 EDTA, 1% Triton-X-100 and 1x phosphatase and protease inhibitors). Lysates were incubated on ice (15 minutes), sonicated, and cleared by centrifugation at 17,000 g . Anti-FLAG – agarose beads (Sigma Aldrich) were prepared by washing 3x in wash buffer ($mmol/L^{-1}$: 50 Tris-HCL, 150 NaCl and 1 EDTA). Cell lysate was added to the pelleted beads. The IP reactions were incubated for 90 minutes at 4degC with agitation. The pulled down proteins were denatured from the beads using 25 µL of a solution containing 50% 4x lauryl dodecyl sulphate sample buffer, 45% wash buffer, 5% β-mercaptoethanol. The ITGA9-GFP was detected in a western using an anti-GFP antibody (Thermo Scientific cat# A-11120). The ITGA4 proteins were detected in a western using an anti-integrin α4 antibody (Santa Cruz cat# sc-365209).

Recombinant protein production

Plasmid expressing manose-binding protein (MBP)-tagged CCP21 or CCP22 domains of SVEP1, or MBP alone under the control of an iso-propyl-thio-β-glactosidase (IPTG) inducible promoter were transformed into E.Coli BCL21 cells. Transformed cells were grown in lysogeny broth (LB) media containing 100 µg mL^{-1}ampicillin to an optical density of between 0.6 and 0.8 at 600 nm. Protein expression was induced by addition of 0.5 mM IPTG. Cell culture was pelleted, lysed and sonicated with the lysate cleared by centrifuging. The MBP-tagged proteins were immunoprecipitated from the cleared cell lysate using amylose beads (New England Biolabs). The protein was eluted from the beads using an affinity purification column with 10 mM maltose in PBS-T. The elution buffer was exchanged using spin columns with a MW cut-off of 30 KDa. Purified protein was run on a 4-12% Bis tris gel with protein visualised by Coomassie staining

Ιντεγριν α4β1^{+} /α9β1^{+} HEK293 ςελλ λινε γενερατιον

HEK293A cells were transfected with 2 µg integrin-α4 plasmid using lipofectamine 2000 (Thermofisher) and selected using 800 µg mL^{-1} geneticin 48 hours post transfection. Cells were diluted to single cell to isolate individual colonies and clones expressing integrin-α4 were identified using an integrin-α4 antibody (Santa Cruz cat# sc-365209). HEK293A cells were transfected using the NEPA21 Electroporator system (Nepagene). Cells were transfected with 10 µg integrin α9-GFP plasmid in OptimMEM®. After 48 hours, cells were selected using 500 µg mL^{-1} geneticin selection. Cells were diluted to single cell to isolate individual clones, with clones expressing integrin α9-GFP identified by fluorescent microscopy.

Recombinant protein cell binding assay

100 nM recombinant MBP control, MBP tagged-CCP21 or MBP tagged-CCP22 was coated onto a 96 well tissue culture plate. Non-specific binding was blocked using DMEM containing 10 mg/mL bovine serum albumin, 10 mM HEPES. 20,000 HEK293 control (α4/α9^{-}), integrin α4β1 (α4β1^{+}), or α9β1 overexpressing

($\alpha9\beta1^+$) cells were seeded onto the coated plates in blocking buffer. The $\alpha4\beta1^+$ cells were incubated for 3 hours and the $\alpha9\beta1^+$ cells were incubated for 30 minutes at 370C. and incubated at 370C for 30 minutes. Plates were washed, fixed with 4% PFA and visualised using DAPI. The number of adhered cells was measured using Fiji.

Statistical Analysis

Histograms and q-q plots were used to evaluate the assumption of normality. Continuous data were presented as mean (SD). The independent samples Student's t-test was used to evaluate the differences between two groups, whilst the one-way ANOVA was used to evaluate differences among >2 experimental groups followed by Tukey's multiple comparisons test. To examine the effect of genotype on tension over extended U46619 concentrations we fitted mixed-effects models, implementing the restriction maximum likelihood estimation, with random intercepts for the different mice. Interactions of the genotype with the different levels of concentration were tested. To decide upon the inclusion of the interaction term we used the Bayesian information criterion (BIC). The interaction term was kept in the model if it produced a smaller BIC value compared to a model with no interaction term. For the models with the interaction term this meant that the genotype effect on vessel tension was not always constant, therefore it varied according to the levels of the U46619 concentration (i.e., dependent of vasoconstrictor concentration: Fig. 5C, 6A, 6B, 6C & 6D). For the models with no interaction term this meant that the genotype effect on vessel tension was independent on the vasoconstrictor concentration (Fig. 5A, 5B, 5D & SF. 10 E). Point estimates are stated in text, whilst the 95% confidence intervals (95% CI) are plotted in the relevant figures. In all analyses, the significance level was set at 5%. Data were analysed using Prism software (GraphPad version 8.1.2., GraphPad Software Inc.) and Stata 16 (StataCorp, 2019. Stata Statistical Software: Release 16. College Station, TX: StataCorp LLC.).

Hosted file

`image18.emf` available at https://authorea.com/users/736210/articles/712029-svep1-regulates-gpcr-mediated-vasoconstriction-via-integrin-%CE%B19%CE%B21-and-%CE%B14%CE%B21

Table S1: Primer sequences

Hosted file

`image19.emf` available at https://authorea.com/users/736210/articles/712029-svep1-regulates-gpcr-mediated-vasoconstriction-via-integrin-%CE%B19%CE%B21-and-%CE%B14%CE%B21

Table S2: Antibody suppliers and catalogue numbers

1 Webb, R. C. Smooth muscle contraction and relaxation. *Adv Physiol Educ* **27** , 201-206, doi:10.1152/advan.00025.2003 (2003).

2 Brozovich, F. V. *et al.* Mechanisms of Vascular Smooth Muscle Contraction and the Basis for Pharmacologic Treatment of Smooth Muscle Disorders. *Pharmacol Rev* **68** , 476-532, doi:10.1124/pr.115.010652 (2016).

3 Mogford, J. E., Davis, G. E., Platts, S. H. & Meininger, G. A. Vascular smooth muscle alpha v beta 3 integrin mediates arteriolar vasodilation in response to RGD peptides. *Circulation research***79** , 821-826 (1996).

4 Waitkus-Edwards, K. R. *et al.* alpha(4)beta(1) Integrin activation of L-type calcium channels in vascular smooth muscle causes arteriole vasoconstriction. *Circulation research* **90** , 473-480 (2002).

5 Wu, X. *et al.* Modulation of calcium current in arteriolar smooth muscle by alphav beta3 and alpha5 beta1 integrin ligands. *The Journal of cell biology* **143** , 241-252 (1998).

6 Mogford, J. E., Davis, G. E. & Meininger, G. A. RGDN peptide interaction with endothelial alpha5beta1 integrin causes sustained endothelin-dependent vasoconstriction of rat skeletal muscle arterioles. *The Journal*

of clinical investigation **100** , 1647-1653, doi:10.1172/JCI119689 (1997).

7 Wu, X., Davis, G. E., Meininger, G. A., Wilson, E. & Davis, M. J. Regulation of the L-type calcium channel by alpha 5beta 1 integrin requires signaling between focal adhesion proteins. *The Journal of biological chemistry* **276** , 30285-30292, doi:10.1074/jbc.M102436200 (2001).

8 Chen, C. *et al.* Integrin alpha9beta1 in airway smooth muscle suppresses exaggerated airway narrowing. *The Journal of clinical investigation* **122** , 2916-2927, doi:10.1172/JCI60387 (2012).

9 Sato-Nishiuchi, R. *et al.* Polydom/SVEP1 is a ligand for integrin alpha9beta1. *The Journal of biological chemistry***287** , 25615-25630, doi:10.1074/jbc.M112.355016 (2012).

10 Shur, I., Socher, R., Hameiri, M., Fried, A. & Benayahu, D. Molecular and cellular characterization of SEL-OB/SVEP1 in osteogenic cells in vivo and in vitro. *Journal of cellular physiology***206** , 420-427, doi:10.1002/jcp.20497 (2006).

11 Gilges, D. *et al.* Polydom: a secreted protein with pentraxin, complement control protein, epidermal growth factor and von Willebrand factor A domains. *The Biochemical journal* **352 Pt 1** , 49-59 (2000).

12 Schwanzer-Pfeiffer, D., Rossmanith, E., Schildberger, A. & Falkenhagen, D. Characterization of SVEP1, KIAA, and SRPX2 in an in vitro cell culture model of endotoxemia. *Cellular immunology***263** , 65-70, doi:10.1016/j.cellimm.2010.02.017 (2010).

13 Karpanen, T. *et al.* An Evolutionarily Conserved Role for Polydom/Svep1 During Lymphatic Vessel Formation. *Circulation research* **120** , 1263-1275, doi:10.1161/CIRCRESAHA.116.308813 (2017).

14 Morooka, N. *et al.* Polydom Is an Extracellular Matrix Protein Involved in Lymphatic Vessel Remodeling. *Circulation research***120** , 1276-1288, doi:10.1161/CIRCRESAHA.116.308825 (2017).

15 Samuelov, L. *et al.* SVEP1 plays a crucial role in epidermal differentiation. *Experimental dermatology* **26** , 423-430, doi:10.1111/exd.13256 (2017).

16 Chen, L. *et al.* The novel miR-1269b-regulated protein SVEP1 induces hepatocellular carcinoma proliferation and metastasis likely through the PI3K/Akt pathway. *Cell Death Dis* **11** , 320, doi:10.1038/s41419-020-2535-8 (2020).

17 Glait-Santar, C., Pasmanik-Chor, M. & Benayahu, D. Expression pattern of SVEP1 alternatively-spliced forms. *Gene* **505** , 137-145, doi:10.1016/j.gene.2012.05.015 (2012).

18 Myocardial Infarction, G. *et al.* Coding Variation in ANGPTL4, LPL, and SVEP1 and the Risk of Coronary Disease. *The New England journal of medicine* **374** , 1134-1144, doi:10.1056/NEJMoa1507652 (2016).

19 Myocardial Infarction Genetics, C. E. C. I. Coding Variation in ANGPTL4, LPL, and SVEP1 and the Risk of Coronary Disease. *New England Journal of Medicine* **374** , 1134-1144, doi:doi:10.1056/NEJMoa1507652 (2016).

20 Levy, D. *et al.* Genome-wide association study of blood pressure and hypertension. *Nature genetics* **41** , 677-687, doi:10.1038/ng.384 (2009).

21 Evangelou, E. *et al.* Genetic analysis of over 1 million people identifies 535 new loci associated with blood pressure traits.*Nature genetics* **50** , 1412-1425, doi:10.1038/s41588-018-0205-x (2018).

22 Palmer, E. L., Ruegg, C., Ferrando, R., Pytela, R. & Sheppard, D. Sequence and tissue distribution of the integrin alpha 9 subunit, a novel partner of beta 1 that is widely distributed in epithelia and muscle. *The Journal of cell biology* **123** , 1289-1297, doi:10.1083/jcb.123.5.1289 (1993).

23 Jung, I. H. *et al.* SVEP1 is a human coronary artery disease locus that promotes atherosclerosis. *Science translational medicine* **13** , doi:10.1126/scitranslmed.abe0357 (2021).

24 Winkler, M. J. *et al.* Functional investigation of the coronary artery disease gene SVEP1. *Basic Res Cardiol* **115** , 67, doi:10.1007/s00395-020-00828-6 (2020).

25 Ihara, E. *et al.* Mechanism of down-regulation of L-type Ca(2+) channel in the proliferating smooth muscle cells of rat aorta. *J Cell Biochem* **87** , 242-251, doi:10.1002/jcb.10295 (2002).

26 Widdop, S., Daykin, K. & Hall, I. P. Expression of muscarinic M2 receptors in cultured human airway smooth muscle cells. *American journal of respiratory cell and molecular biology* **9** , 541-546, doi:10.1165/ajrcmb/9.5.541 (1993).

27 Halayko, A. J., Salari, H., Ma, X. & Stephens, N. L. Markers of airway smooth muscle cell phenotype. *Am J Physiol* **270** , L1040-1051, doi:10.1152/ajplung.1996.270.6.L1040 (1996).

28 Maguire, E. M., Xiao, Q. & Xu, Q. Differentiation and Application of Induced Pluripotent Stem Cell-Derived Vascular Smooth Muscle Cells.*Arteriosclerosis, thrombosis, and vascular biology* **37** , 2026-2037, doi:10.1161/ATVBAHA.117.309196 (2017).

29 Nelson, M. T. & Quayle, J. M. Physiological roles and properties of potassium channels in arterial smooth muscle. *Am J Physiol***268** , C799-822, doi:10.1152/ajpcell.1995.268.4.C799 (1995).

30 Ringvold, H. C. & Khalil, R. A. Protein Kinase C as Regulator of Vascular Smooth Muscle Function and Potential Target in Vascular Disorders. *Adv Pharmacol* **78** , 203-301, doi:10.1016/bs.apha.2016.06.002 (2017).

31 Yan, H. *et al.* Mechanisms of U46619-induced contraction in mouse intrarenal artery. *Clin Exp Pharmacol Physiol* **46** , 643-651, doi:10.1111/1440-1681.13087 (2019).

32 Alapati, V. R. *et al.* Mechanisms of U46619- and 5-HT-induced contraction of bovine pulmonary arteries: role of chloride ions.*British journal of pharmacology* **151** , 1224-1234, doi:10.1038/sj.bjp.0707338 (2007).

33 Bauer, J. *et al.* ANG II- and TxA(2)-induced mesenteric vasoconstriction in rats is mediated by separate cell signaling pathways. *Am J Physiol* **277** , H1-7, doi:10.1152/ajpheart.1999.277.1.H1 (1999).

34 Wilson, D. P., Susnjar, M., Kiss, E., Sutherland, C. & Walsh, M. P. Thromboxane A2-induced contraction of rat caudal arterial smooth muscle involves activation of Ca2+ entry and Ca2+ sensitization: Rho-associated kinase-mediated phosphorylation of MYPT1 at Thr-855, but not Thr-697.*The Biochemical journal* **389** , 763-774, doi:10.1042/BJ20050237 (2005).

35 Zhang, Z., Baron, R. & Horne, W. C. Integrin engagement, the actin cytoskeleton, and c-Src are required for the calcitonin-induced tyrosine phosphorylation of paxillin and HEF1, but not for calcitonin-induced Erk1/2 phosphorylation. *The Journal of biological chemistry***275** , 37219-37223, doi:10.1074/jbc.M001818200 (2000).

36 Slack, B. E. Tyrosine phosphorylation of paxillin and focal adhesion kinase by activation of muscarinic m3 receptors is dependent on integrin engagement by the extracellular matrix. *Proceedings of the National Academy of Sciences of the United States of America***95** , 7281-7286 (1998).

37 Min, J. *et al.* Src modulates contractile vascular smooth muscle function via regulation of focal adhesions. *Journal of cellular physiology* **227** , 3585-3592, doi:10.1002/jcp.24062 (2012).

38 Kwon, M. S. *et al.* Calreticulin couples calcium release and calcium influx in integrin-mediated calcium signaling. *Molecular biology of the cell* **11** , 1433-1443, doi:10.1091/mbc.11.4.1433 (2000).

39 Davis, G. E. Matricryptic sites control tissue injury responses in the cardiovascular system: relationships to pattern recognition receptor regulated events. *Journal of molecular and cellular cardiology***48** , 454-460, doi:10.1016/j.yjmcc.2009.09.002 (2010).

40 Davis, G. E., Bayless, K. J., Davis, M. J. & Meininger, G. A. Regulation of tissue injury responses by the exposure of matricryptic sites within extracellular matrix molecules. *The American journal of pathology*

156 , 1489-1498, doi:10.1016/S0002-9440(10)65020-1 (2000).

41 Martinez-Lemus, L. A. *et al.* Integrins as unique receptors for vascular control. *Journal of vascular research* **40** , 211-233, doi:10.1159/000071886 (2003).

42 Hansson, G. K. Inflammation, atherosclerosis, and coronary artery disease. *The New England journal of medicine* **352** , 1685-1695, doi:10.1056/NEJMra043430 (2005).

43 Blaise, S. *et al.* Elastin-derived peptides are new regulators of insulin resistance development in mice. *Diabetes* **62** , 3807-3816, doi:10.2337/db13-0508 (2013).

44 Galis, Z. S. & Khatri, J. J. Matrix metalloproteinases in vascular remodeling and atherogenesis: the good, the bad, and the ugly.*Circulation research* **90** , 251-262 (2002).

45 Westman, P. C. *et al.* Inflammation as a Driver of Adverse Left Ventricular Remodeling After Acute Myocardial Infarction. *Journal of the American College of Cardiology* **67** , 2050-2060, doi:10.1016/j.jacc.2016.01.073 (2016).

46 Hill, J. W. & Nemoto, E. M. Matrix-derived inflammatory mediator N-acetyl proline-glycine-proline is neurotoxic and upregulated in brain after ischemic stroke. *Journal of neuroinflammation* **12** , 214, doi:10.1186/s12974-015-0428-z (2015).

47 Kessler, T. *et al.* ADAMTS-7 inhibits re-endothelialization of injured arteries and promotes vascular remodeling through cleavage of thrombospondin-1. *Circulation* **131** , 1191-1201, doi:10.1161/CIRCULATIONAHA.114.014072 (2015).

48 Coronary Artery Disease Genetics, C. A genome-wide association study in Europeans and South Asians identifies five new loci for coronary artery disease. *Nature genetics* **43** , 339-344, doi:10.1038/ng.782 (2011).

49 Reilly, M. P. *et al.* Identification of ADAMTS7 as a novel locus for coronary atherosclerosis and association of ABO with myocardial infarction in the presence of coronary atherosclerosis: two genome-wide association studies. *Lancet* **377** , 383-392, doi:10.1016/S0140-6736(10)61996-4 (2011).

50 Schunkert, H. *et al.* Large-scale association analysis identifies 13 new susceptibility loci for coronary artery disease.*Nature genetics* **43** , 333-338, doi:10.1038/ng.784 (2011).

51 Takahashi, K. *et al.* Induction of pluripotent stem cells from adult human fibroblasts by defined factors. *Cell* **131** , 861-872, doi:10.1016/j.cell.2007.11.019 (2007).

52 Bayless, K. J. & Davis, G. E. Identification of dual alpha 4beta1 integrin binding sites within a 38 amino acid domain in the N-terminal thrombin fragment of human osteopontin. *The Journal of biological chemistry* **276** , 13483-13489, doi:10.1074/jbc.M011392200 (2001).

53 Davis, G. E. Affinity of integrins for damaged extracellular matrix: alpha v beta 3 binds to denatured collagen type I through RGD sites.*Biochemical and biophysical research communications* **182** , 1025-1031 (1992).

54 Schindelin, J. *et al.* Fiji: an open-source platform for biological-image analysis. *Nature methods* **9** , 676-682, doi:10.1038/Nmeth.2019 (2012).